Dynamics and transitions of the coupled Lorenz system

Hsien-Chen Ma, Chien-Chong Chen,* and Bai-Wei Chen
Department of Chemical Engineering, National Chung Cheng University, Chia-Yi 621, Taiwan
(Received 6 February 1997)

In this paper, we are interested in a very simple and fundamental question: Is the dynamics of a coupled chaotic system always chaotic? It is found that in addition to the expected complicated chaos and hyperchaos, two identical Lorenz systems starting at different initial conditions and coupling together via nonfeedback-type interactions can also exhibit simple dynamics such as fixed points, limit cycles, and tori in wide parametric ranges of coupling constants. Also, in the parametric space of coupling constants, four distinct routes of dynamical transitions are found for this simple coupled system. Along the route of dynamical transitions, intermittence, sideband instability, and nonlinear interactions of dynamical modes are all involved. [S1063-651X(97)06108-4]

PACS number(s): 05.45.+b

I. INTRODUCTION

Since the introduction of chaos several decades ago, the dynamical behavior of coupled oscillators, as well as coupled chaotic system, has been studied extensively. It can be found from the literature that several research directions pertinent to the coupled chaotic systems have been proposed. First, coupled chaotic systems are used for communication by synchronization of two chaotic circuits [1–4]. Basically, chaotic signals of a driving system serve as external forcings of the driven system such that output signals of the driven system are synchronized with the driving signals. Although the driving and driven signals are synchronized and are nearly the same, both systems remain chaotic, i.e., the dynamics of this coupled chaotic system is chaotic or hyperchaotic. Next, chaotic coupling is also utilized to achieve control [5–7]. This control scheme is different from the pioneering Ott-Grebogi-Yorke method since two or more chaotic systems are involved. It is essentially a linear or nonlinear feedback control approach. A slave chaotic system is forced by signals of a master chaotic system as well as its own signals, which are the feedback terms. By adjusting the feedback control gains, the slave system is controlled such that its behavior is identical to the master system. Our personal reasoning for this approach is that the feedback control first destroys the chaotic dynamics of the slave system such that all the eigenvalues of the linearized slave system have negative real parts. The master system then easily takes control of the slave system by chaotic forcings (couplings).

Another direction to study the coupled chaotic systems focuses on their dynamical behavior. Intuitively, for chaotic systems coupled together, hyperchaotic attractors are naturally expected and are easily obtained for coupled chaotic circuits [8], van der Pol equations [9], and Duffing oscillators [10]. In Ref. [10] a scaling law to detect the transition from chaos to hyperchaos has been proposed. It is not surprising that the resulting dynamics of coupled chaotic systems is the more complex hyperchaos because we experience from time to time that two complicated systems mixed together become more complex. In addition to the hyperchaos, simple dynamics such as fixed points and limit cycles can also be obtained by the feedback-type interactions between two chaotic systems [11]. However, these results are not surprising either. As we mentioned earlier, feedback control could disable the chaotic nature of chaotic systems. Therefore, by suitably adjusting the feedback gains, which are also the coupling constants, one can easily obtain simple nonchaotic dynamics for the coupled chaotic systems. From the above results reported in the literature, we can conclude that if the interactions between two chaotic systems are not of the feedback type, the dynamics of coupled chaotic systems is chaotic or hyperchaotic. Simpler dynamics is only possible if the coupling between two chaotic systems is feedback control. Here we are interested in a very simple and fundamental question: If two chaotic systems are coupled together via the nonfeedback-type interactions, is it possible that the dynamics of this coupled chaotic system becomes simpler, i.e., nonchaotic? In this paper two identical Lorenz systems starting at different initial conditions coupled by nonfeedback-type interactions are studied. We found that, depending on the combinations of coupling constants, nonchaotic dynamics could be obtained for this simple coupled system as well as the expected chaos and hyperchaos. Moreover, four distinct transitions, on which complicated dynamics evolves to simpler dynamics, are observed as coupling constants are varied.

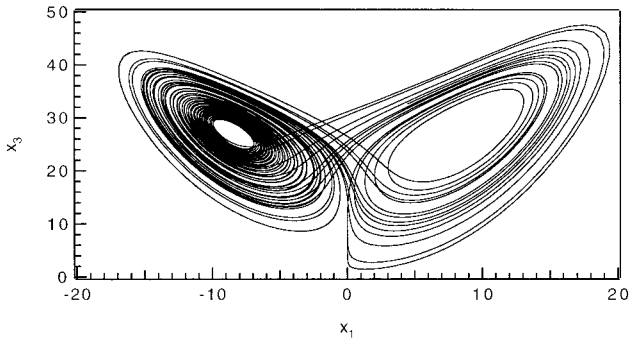

FIG. 1. Chaotic attractor of the Lorenz system described by Eq. (1).

*Author to whom correspondence should be addressed. Electronic address: chmccc@ccunix.ccu.edu.tw.

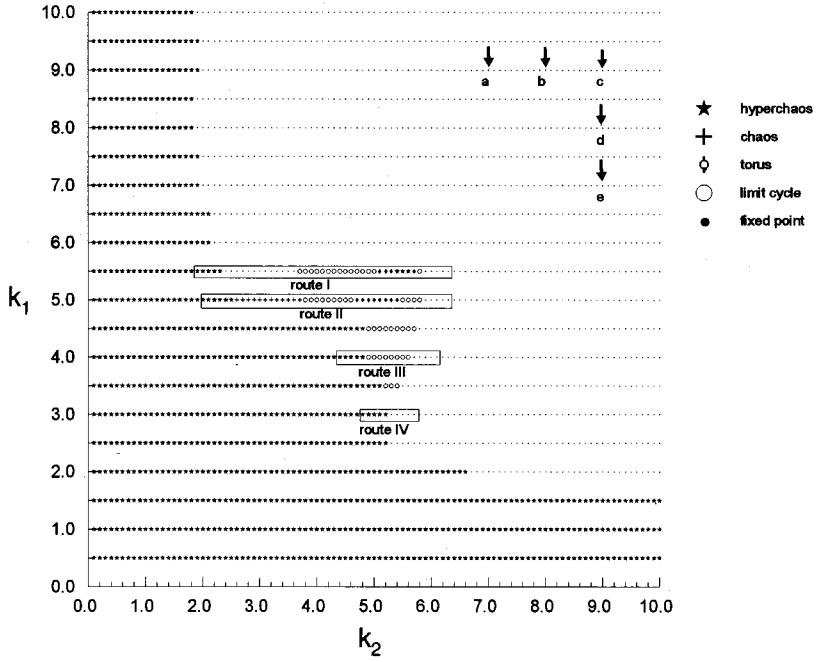

FIG. 2. Dynamics of the coupled Lorenz system of Eqs. (2) in the parametric space of the coupling constants k_1 and k_2.

II. THE COUPLED LORENZ SYSTEM

Because we are interested in whether or not the dynamics of the coupled chaotic system can become nonchaotic, the standard Lorenz system [12] is selected as our modal system since its dynamical behavior is well documented [13]. The Lorenz system is described by the differential equations

$$\begin{aligned} \dot{x}_1 &= \sigma(x_2 - x_1), \\ \dot{x}_2 &= r x_1 - x_1 x_3 - x_2, \\ \dot{x}_3 &= x_1 x_2 - b x_3, \end{aligned} \tag{1}$$

with parametric values $(\sigma, r, b) = (10, \frac{8}{3}, 28)$. The Lorenz system given in Eq. (1) behaves chaotically, as shown in Fig. 1. Two identical Lorenz systems starting at different initial conditions are coupled together and the coupling between two Lorenz systems is a bidirectionally linear interaction. The resulting coupled system reads

$$\begin{aligned} \dot{x}_1 &= \sigma(x_2 - x_1) + k_1 y_1, \\ \dot{x}_2 &= r x_1 - x_1 x_3 - x_2, \\ \dot{x}_3 &= x_1 x_2 - b x_3; \end{aligned} \tag{2a}$$

$$\begin{aligned} \dot{y}_1 &= \sigma(y_2 - y_1) + k_2 x_1, \\ \dot{y}_2 &= r y_1 - y_1 y_3 - y_2, \\ \dot{y}_3 &= y_1 y_2 - b y_3, \end{aligned} \tag{2b}$$

where k_1 and k_2 are coupling constants. The coupling terms $k_1 y_1$ and $k_2 x_1$ selected are of the simplest case and are not mandatory. Of course, one can select other types of interactions. However, for our purpose to see whether the coupled chaotic system will result in simpler dynamics, the simplest linear interaction will suffice. It is also noted that although the two Lorenz systems in Eqs. (2a) and (2b) are the same, starting at distinct initial conditions yields different corresponding x and y even though the large-time behaviors of the two systems are in the same chaotic attractor. Therefore, the coupling terms are not the feedback type. We can also confirm that this coupled system does not contain feedback interactions by checking the resulting dynamics. If there are

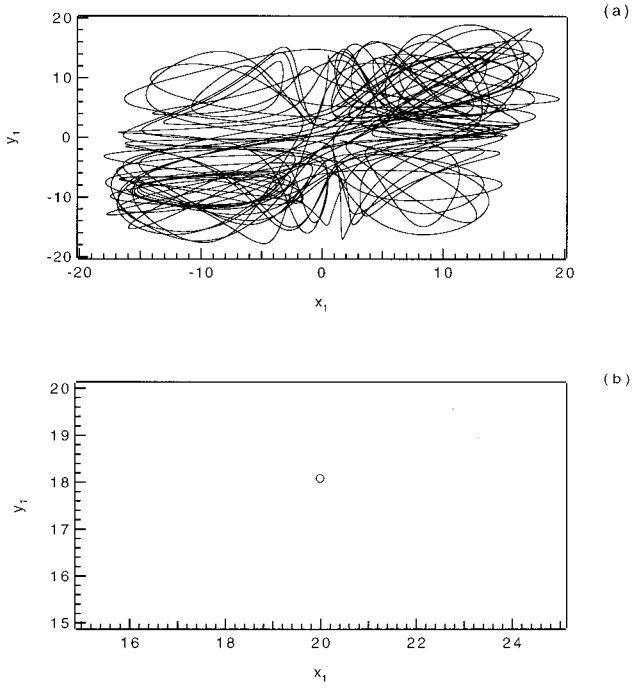

FIG. 3. Phase plots of (a) a hyperchaotic attractor when $k_1 = 3$ and $k_2 = 1$ and (b) a fixed-point attractor when $k_1 = 9$ and $k_2 = 7$. Note that x_1 and y_1 are not synchronized.

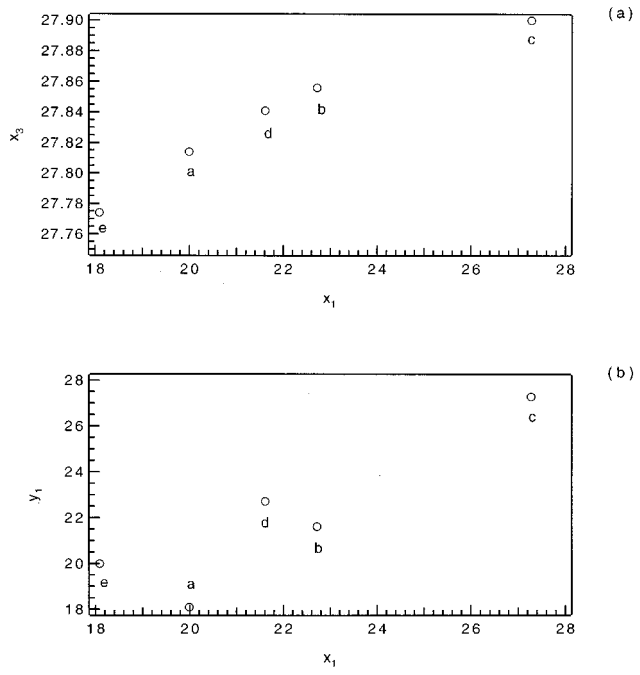

FIG. 4. Amplitudes of states x_1, x_3, and y_1 of the fixed-point attractors in (a) x_3-x_1 and (b) y_1-x_1 phase spaces approximately vary linearly with respect to the coupling constants. The corresponding coupling strengths of points a, b, c, d, and e are marked on Fig. 2.

TABLE I. Four distinct routes of dynamical transitions. Routes are marked on Fig. 2.

Route	Dynamical variations
I	hyperchaos↔fixed point↔limit cycle↔ torus↔hyperchaos↔torus ↔limit cycle↔ fixed point
II	hyperchaos↔chaos↔limit cycle↔torus↔limit cycle ↔fixed point
III	hyperchaos↔limit cycle↔fixed point
IV	hyperchaos↔fixed point

feedback controls involved in Eqs. (2), then $x_1(t)=y_1(t)$ and Eqs. (2a) and (2b) will become identical such that $\mathbf{x}(t)=\mathbf{y}(t)$. We will show later that $\mathbf{x}(t)$ and $\mathbf{y}(t)$ are not the same.

Several simple and standard dynamical tools are applied to study the dynamics of the coupled Lorenz system described by Eqs. (2). First, the dynamical behaviors of this coupled system are first obtained by solving Eqs. (2) using a double-precision fourth-order Runge-Kutta method. By varying the magnitudes of the coupling constants k_1 and k_2, we can see whether or not the dynamical behavior of the coupled system is nonchaotic. With the time series available, phase plots can reveal the topological structures of the resulting attractors. Next, the linear stability analysis is carried out around the steady states of Eqs. (2). If the dynamics of the coupled system is a simple fixed point, all the eigenvalues of

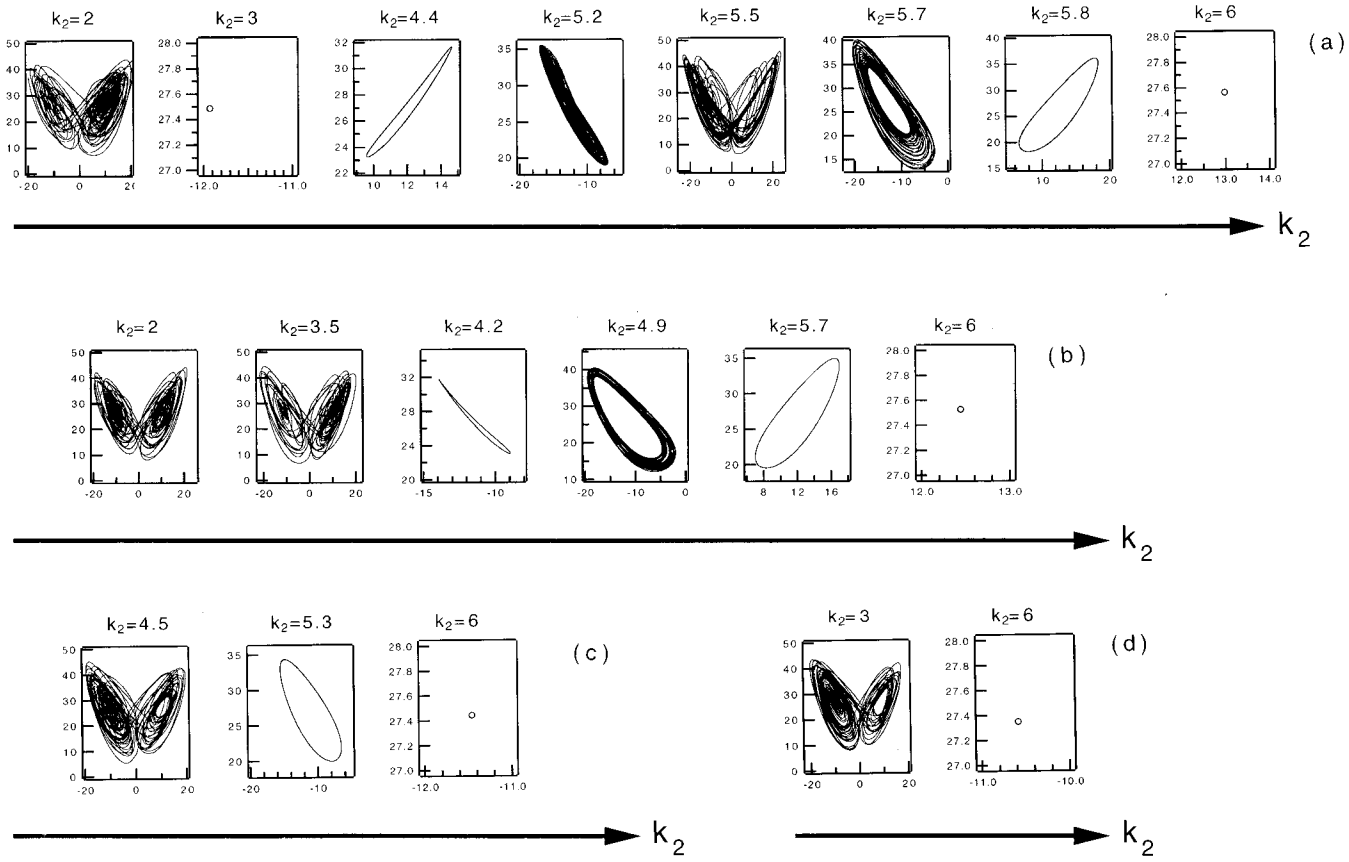

FIG. 5. Typical dynamical behaviors in the x_3-x_1 phase space along four distinct routes marked on Fig. 2. (a), (b), (c), and (d) are the first, the second, the third, and the fourth route, respectively.

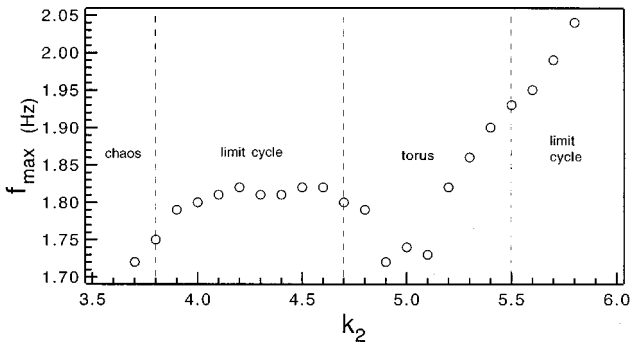

FIG. 6. Variations of the dominant frequency along the second route.

the Jacobian matrix will have negative real parts. On the other hand, if the time series obtained from Eqs. (2) is not a simple steady state but rather a periodic motion, the fast Fourter fransform (FFT) can be applied to that time series to determine the complexity of the periodic orbit by counting the number of peaks in the power spectrum. Moreover, if the obtained dynamics is still chaotic, the number of positive Lyapunov exponents can indicate that this attractor is chaotic or hyperchaotic by computing the Lyapunov spectrum from the chaotic time series. One positive Lyapunov exponent corresponds to the chaotic attractor, while two or more positive Lyapunov exponents indicate a hyperchaotic attractor.

III. NONCHAOTIC AND CHAOTIC DYNAMICS

As stated in the preceding section, we adopt the simple dynamical tools to study how the dynamical behavior of the coupled Lorenz system varies with the coupling constants. We focus our attention on the search for the nonchaotic dynamics. The values of coupling constants k_1 and k_2 both range from 0 to 10. In the interval [0, 10], k_1 and k_2 vary every 0.5 and 0.1 steps, respectively. Although resolution in the k_1-k_2 parametric space is not very fine, it is good enough to determine whether or not this coupled Lorenz system could behave nonchaotically. Figure 2 shows that the

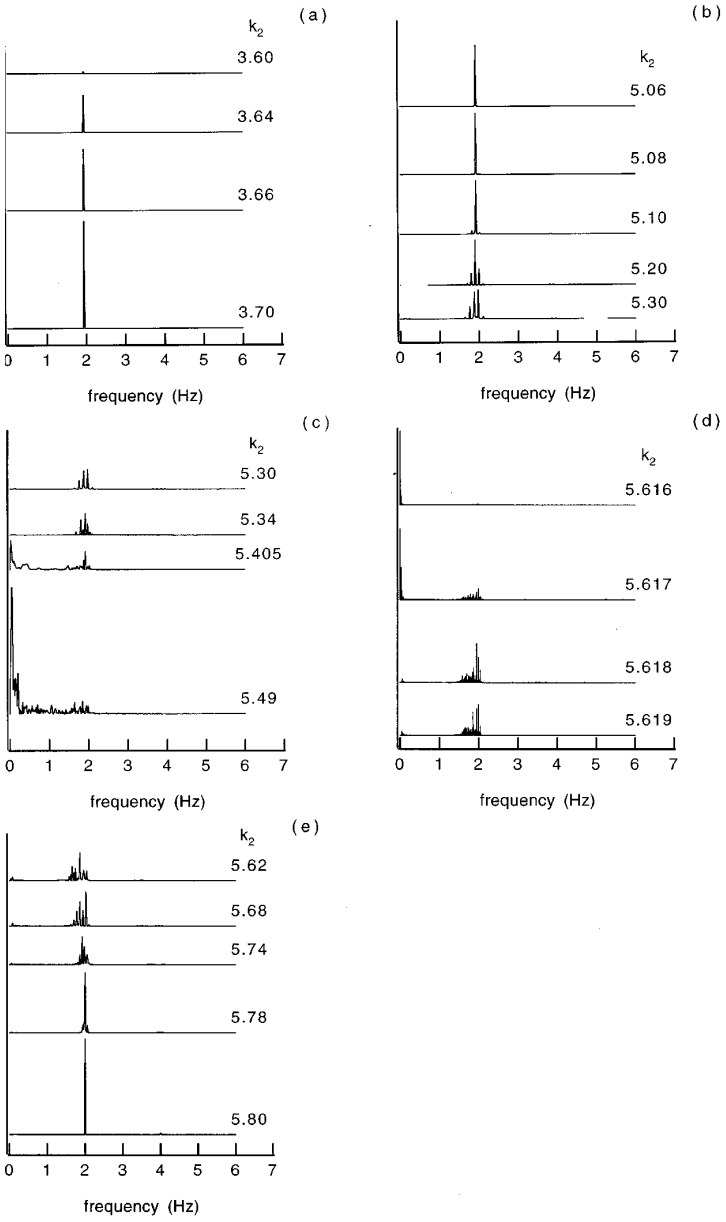

FIG. 7. Power spectra in the processes of major dynamical transitions along the first route: (a) the fixed point to the limit cycle, (b) the limit cycle to the torus, (c) the torus to hyperchaos, (d) hyperchaos to the torus, and (e) the torus to the limit cycle.

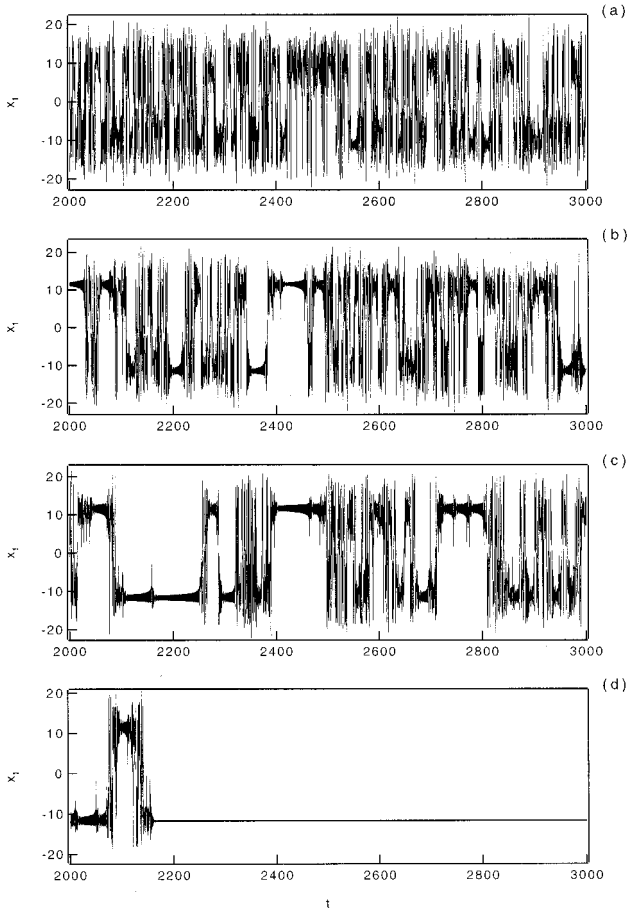

FIG. 8. Time series of the hyperchaos–fixed-point transition on the first route show the intermittency behavior (a) $k_2=0.8$, (b) $k_2=1.6$, (c) $k_2=2.304$, and (d) $k_2=2.3072$.

dynamical behavior of the coupled Lorenz system described by Eqs. (2) is very rich in the k_1-k_2 parametric space. It is clearly seen that in addition to the expected chaos or hyperchaos, simple dynamics such as fixed points, limit cycles, and tori are observed. This answers our question: The dynamics of a coupled chaotic system with nonfeedback-type interactions can indeed become nonchaotic. Also, as is evident in Fig. 2, the nonchaotic dynamics is not a rare exception; they are located in a large upper triangular region of the parametric space. On the other hand, chaos and hyperchaos appear at the lower triangle. Chaotic characteristics of the individual Lorenz systems are sustained when coupling strengths are small. This suggests that only fairly large interactions could suppress the chaos. Figure 3 shows hyperchaos for $(k_1,k_2)=(3,1)$ and a simple fixed point for $(k_1,k_2)=(7,9)$. The corresponding states x_1 and y_1 in the respective Lorenz systems are not synchronized and are not the same in both cases. This confirms that the couplings in Eqs. (2) are not feedback controls, although two identical Lorenz systems are coupled together. For the fixed-point region in Fig. 2, an increase of the coupling strengths can raise the magnitudes of states x and y. Figure 4 shows that the amplitudes of x_1, x_3 and y_1 become larger in the direction of increasing k_1 or k_2.

IV. TRANSITIONS

We have shown that nonchaotic dynamics does exist for the coupled Lorenz system and that hyperchaotic and fixed-point attractors occupy the most area in the parametric space in Fig. 2. In addition to the above two extreme dynamics, other dynamics such as limit cycles, tori, and chaos are also available. The main focus here is not on that this coupled system is capable of displaying abundant dynamical behavior, but on the dynamical transitions when the coupling constants are varied. As shown in Fig. 2, if k_1 is kept constant, we can see that the dynamics is hyperchaotic for small k_2's and fixed points for large k_2's. As k_2 increases from 0, the dynamics of the coupled systems switches directly from the hyperchaotic to the fixed-point attractor for large and small k_1. But, in the medial k_1, there exists an intermediate dynamics between these two extremes of hyperchao and the fixed point. It is noted that fixed-point dynamics is confirmed by the ''flat'' time series and by the Jacobian matrix having all eigenvalues with negative real parts, while hyperchaos is ensured by two positive Lyapunov exponents computed from the time series.

In the parametric values of k_1 and k_2 studied, we have found four distinct routes of dynamical transitions and have marked them on Fig. 2. Table I summarizes these four different routes. Note that since our partitions of k_1 and k_2 are not very fine, it will not be surprising to obtain more routes if finer partitions on coupling constants are carried out. Nevertheless, under the current partition, it is amazing to see that this simple coupled system is capable of displaying rich dynamical transitions. Moreover, several routes cannot be found in the literature. From the literature [14,15] the transitions to chaos could be triggered by (a) a local bifurcation, which includes periodic doubling, quasiperiodicity, and intermittence, or (b) a global bifurcation, which can be a chaotic transience or a crisis. In addition to the above well-known routes, a different route via a torus breakdown [16] is also reported. We will state why the observed transitions differ from those in the literature later. First, representative dynamical behaviors along the four routes observed are shown in Fig. 5, in which dynamical transitions are seen clearly. Next, following the different routes, FFT analyses of the resulting time series are carried out to obtain the power spectrum. For simplicity, we consider the variations of the dominant frequency on the second route. The dominant frequency $f_{\max}$ along the second route is given in Fig. 6. As k_2 switches from the chaotic to the limit-cycle region, the magnitude of $f_{\max}$ increases. $f_{\max}$ remains roughly constant in the limit-cycle region and then becomes smaller in the first half of the torus window. When k_2 is in the second half of the torus window and in the limit-cycle regime, $f_{\max}$ increases monotonically.

In addition to the variations of the dominant frequency, the FFT analysis also reveals the underlying causes for the transitions. As shown in Table I, the first route has the most variations of the dynamical behavior so that power spectra along this route are analyzed in detail. Power spectra near the switches of dynamics are shown in Fig. 7. We will discuss the first hyperchaos–fixed-point transition later because it is difficult to gain any insight from the variations of the broadband power spectra. The next major dynamical change is from the fixed point to the limit cycle. In the very beginning of the limit cycle ($k_2=3.6$), a sole tiny peak appears at 1.94. When k_2 increases, this peak starts to grow while the frequency stays approximately at the same value as in Fig. 7(a).

This means that the size of the limit cycle in the limit-cycle region becomes bigger and bigger as k_2 increases. Next, the variations of the power spectra in the limit-cycle–torus window is considered. As shown in Fig. 7(b), when k_2 moves from 5.08 to 5.10, there are two sideband peaks, which exist in a pair, centered at the original dominant peak. The transition from the limit cycle to the torus of this type corresponds to the sideband instability [17]. A further increase of k_2 to 5.12 results in a decrease of the main peak, an increase of sideband peaks, and the creation of another two sideband peaks. This is due to the nonlinear interactions between the main peak and the two sideband peaks. Also, because of the resonant conditions, the frequencies of two new sideband peaks are the linear combinations of the dominant peak and two old sideband peaks. Note that although it is not clearly visible in Fig. 7(b), there exists a superharmonic peak with approximately twice the dominant frequency for various k_2's. However, this superharmonic mode remains inactive such that the period-doubling scenario does not occur. If we continue increasing k_2, a wave pocket is formed at $k_2 = 5.34$ in Fig. 7(c) and it is later destabilized at $k_2 = 5.405$ to yield large low-frequency peaks such that a broadband frequency structure starts to emerge. This broadband structure is fully developed with a giant low-frequency peak at $k_2 = 5.49$ and the dynamics of the coupled system is switched back to hyperchaos.

The second part of the transition from hyperchaos to simpler dynamics is basically a reverse process of the first part. Figures 7(d) and 7(e) are virtually equivalent to the reverse of Figs. 7(b) and 7(c). From Fig. 2, because the following limit-cycle–fixed-point transition occurs in a very narrow range of k_2, the process of diminishing the amplitude from the limit cycle to the fixed point is difficult to observe. We return now to the first hyperchaos–fixed-point transition. Power spectra along this transition cannot provide meaningful information, so we observe the variations of time series directly. Figure 8 displays the time series before k_2 reaches the fixed-point dynamics. If we view these four time series in the reverse order, i.e., from the direction of the fixed point to hyperchaos, it behaves like the intermittent transition. Summarizing the above results, the dynamical variations along the first route include an intermittent transition, a sideband instability, nonlinear interactions of dynamical modes, and a reverse process of the above phenomena. This rich dynamical transition with only one parameter varied is completely different from those routes to chaos reported in the literature.

V. CONCLUSION

We have shown that the coupling of two identical Lorenz systems starting at different initial conditions via the nonfeedback-type interaction can exhibit a wide variety of dynamical behaviors such as a fixed point, a limit cycle, tori, chaos, and hyperchaos. We show that simple dynamics is possible for the coupled chaotic system with nonfeedback-type interactions. Also, four distinct routes of dynamical transitions are observed for this simple coupled chaotic system. FFT and time series analyses show that intermittence, sideband instability, and nonlinear interactions are involved along the route of dynamical variations. Since this extremely simple coupled chaotic system is capable of providing so many interesting dynamical behaviors, it is expected that more dynamical behaviors are possible if we are dealing with more complex coupled systems and with different types of interactions.

ACKNOWLEDGMENTS

This work is supported by the National Science Council of the Republic of China under Grant No. NSC-86-2214-E-194-003. Thanks are also due to the computing center of National Chung Cheng University for providing the IBM sp2 parallel computers.

[1] L. M. Pecora and T. L. Carroll, Phys. Rev. Lett. **64**, 821 (1990); L. M. Pecora and T. L. Carroll, Phys. Rev. A **44**, 2374 (1991); T. L. Carroll and L. M. Pecora, IEEE Trans. Circuits Syst. **38**, 453 (1991).

[2] S. Hayes, C. Grebogi, E. Ott, and A. Mark, Phys. Rev. Lett. **73**, 1781 (1994).

[3] L. Kocarev and U. Parlitz, Phys. Rev. Lett. **74**, 5028 (1995).

[4] X. Kapitaniak, J. Wojewoda, and J. Brindley, Phys. Lett. A **210**, 283 (1996).

[5] C. W. Wu and L. O. Chua, Int. J. Bifurcation Chaos **4**, 979 (1994).

[6] G. Chen and X. Dong, IEEE Trans. Circuits Syst. **40**, 591 (1993); G. Chen, *ibid.* **40**, 829 (1993).

[7] K. Pyragas, Phys. Lett. A **181**, 203 (1993); C.-C. Chen, C.-H. Tsai, and C.-C. Fu, *ibid.* **194**, 261 (1994).

[8] T. Kapitaniak, L. O. Chua, and G.-Q. Zhong, IEEE Trans. Circuits Syst. **41**, 499 (1994); T. Kapitaniak and L. O. Chua, Int. J. Bifurcation Chaos **4**, 477 (1994).

[9] T. Kapitaniak and W.-H. Steeb, Phys. Lett. A **152**, 33 (1991); T. Kapitaniak, K.-E. Thylwe, I. Cohen, and J. Wojewoda, Chaos Solitons Fractals **5**, 2003 (1995).

[10] T. Kapitaniak, Phys. Rev. E **47**, R2975 (1993).

[11] Y. Liu and L. C. Barbosa, Phys. Lett. A **197**, 13 (1995); A. Stefanski and T. Kapitaniak, *ibid.* **210**, 279 (1996).

[12] E. N. Lorenz, J. Atmos. Sci. **20**, 130 (1963).

[13] C. Sparrow, *The Lorenz Equations: Bifurcation, Chaos, and Strange Attractors* (Springer-Verlag, New York, 1982).

[14] R. Brown, P. Byrant, and H. D. I. Abarbanel, Phys. Rev. A **43**, 2787 (1991); R. Brown, Phys. Rev. E **47**, 3962 (1993).

[15] R. C. Hilborn, *Chaos and Nonlinear Dynamics: An Introduction for Scientists and Engineers* (Oxford University Press, New York, 1994).

[16] T. Matsumoto, L. O. Chua, and T. Tokunaga, IEEE Trans. Circuits Syst. **CAS-34**, 240 (1987).

[17] M. Cheng and H.-C. Chang, Phys. Fluids A **2**, 1364 (1990).